

# Muon capture, continuum random phase approximation and in-medium renormalization of the axial-vector coupling constant

E. Kolbe\* and K. Langanke

*W. K. Kellogg Radiation Laboratory, 106-38*

*California Institute of Technology, Pasadena, California 91125 USA*

P. Vogel

*Physics Department*

*California Institute of Technology, Pasadena, California 91125 USA*

(November 15, 2018)

## Abstract

We use the continuum random phase approximation to describe the muon capture on  $^{12}\text{C}$ ,  $^{16}\text{O}$  and  $^{40}\text{Ca}$ . We reproduce the experimental total capture rates on these nuclei to better than 10% using the free nucleon weak form factors and two different residual interactions. However, the calculated rates for the same residual interactions are significantly lower than the data if the in-medium quenching of the axial-vector coupling constant is employed.

PACS numbers: 24.30.Cz, 23.40.-s, 23.40.Hc

Typeset using REVTeX

---

\*Present address: Physics Department, University of Basel, CH-4056 Basel, Switzerland

The capture of a negative muon from the atomic  $1s$  orbit,

$$\mu^- + (Z, N) \rightarrow \nu_\mu + (Z - 1, N + 1)^* \quad (1)$$

is a semileptonic weak process which has been studied for a long time (see, e.g., the reviews by Walecka [1] or Mukhopadhyay [2] and the earlier references therein). The total capture rate has been measured for many nuclei; in some cases the partial capture rates to specific states in the daughter nucleus have been determined as well.

The nuclear response in muon capture is governed by the momentum transfer which is of the order of muon mass. The energy transferred to the nucleus is restricted from below by the mass difference of the initial and final nuclei, and from above by the muon mass. The phase space and the nuclear response favor lower nuclear excitation energies, thus the nuclear states in the giant resonance region dominate.

Since the experimental data are quite accurate, and the theoretical techniques of evaluating the nuclear response in the relevant regime are well developed, it is worthwhile to see to what extent the capture rates are understood and, based on such comparison, what can one say about possible in-medium renormalization of the various coupling constants. In particular, there are various indications that the axial-vector coupling constant  $g_A$  in nuclear medium is reduced from its free nucleon value of  $g_A = 1.25$  to the value of  $g_A \simeq 1$ . The evidence for such a renormalization comes primarily from the analysis of beta decay between low-lying states of the ( $sd$ ) shell nuclei [3]. In addition, the “missing Gamow-Teller strength” problem, as revealed in the interpretation of the forward angle ( $p, n$ ) charge-exchange reactions [4], is also often quoted as evidence for quenching of  $g_A$ . The Gamow-Teller strength is concentrated in the giant GT resonance at excitation energies not very far from the energies involved in the muon capture, although this latter process is dominated by the transitions to the negative parity spin-dipole states.

Muon capture also depends on the induced pseudoscalar hadronic weak current. At the free nucleon level the corresponding coupling constant is determined by the Goldberger-Treiman relation [5]

$$F_P(q^2) = \frac{2M_p F_A(0)}{m_\pi^2 - q^2} , \quad (2)$$

where  $m_\pi$  is the pion mass and  $F_A(0) \equiv g_A = 1.25$ . (In muon capture one often uses a dimensionless quantity  $g_P = m_\mu F_P(q^2)$  at the relevant momentum transfer  $q^2 \simeq -0.9m_\mu^2$ , such that  $g_P \simeq 8.4$  for free protons.) In nuclear medium  $F_P$  can be again renormalized, and this renormalization does not necessarily obey the Goldberger-Treiman relation [6].

The Continuum Random Phase Approximation (RPA) has been used successfully in the description of the nuclear response to weak and electromagnetic probes [7]. The method combines the usual RPA treatment with the correct description of the continuum nucleon decay channel. We have used this method for calculations of the muon capture processes on  $^{12}\text{C}$ ,  $^{16}\text{O}$ , and  $^{40}\text{Ca}$ . As residual interactions we adopted the finite-range force [8] based on the Bonn potential [9] and the zero-range Landau-Migdal force with the parametrizations for  $^{12}\text{C}$  and  $^{16}\text{O}$  taken from Refs. [10] and [11], respectively. For  $^{40}\text{Ca}$  we used the standard parametrization as, for example, given in Ref. [12]. Note that none of these forces have been adjusted to weak interaction data for these nuclei. In the calculation we evaluate the capture rate at each energy transfer  $\omega$  for each multipole separately. The momentum conservation condition is fulfilled throughout. We also use an accurate relativistic description of the initial bound muon. Form factors and their  $q$ -dependence have been adopted from Ref. [13].

The results of our calculations are summarized in Figs. 1–3, which show the capture rate as a function of excitation energy, and in Table I, which compares the total capture rates with data. The total muon capture rates for  $^{12}\text{C}$  and  $^{16}\text{O}$ , as given in Table I, are defined as the part of the rate where the nucleus in the final state is excited above the particle threshold and therefore decays via particle emission. The experimental entries in Table I were derived by subtracting the partial muon capture rates into the particle bound states (we used the average of the various data sets) from the total capture rates. We would like to point out that most of the capture rate goes to particle-unbound states. In  $^{12}\text{C}$  capture to particle-bound levels (mainly the  $^{12}\text{B}$  ground state) contributes about 16% of the total rate, while in  $^{16}\text{O}$  the bound-state contributions are roughly 10%. As is obvious from Table I,

our calculations reproduce the total muon capture rates into the continuum states very well. For all three nuclei the Bonn potential slightly overestimates the data, however, by less than 10%. The Landau-Migdal force reproduces the continuum data for  $^{12}\text{C}$  and  $^{16}\text{O}$  remarkably well, while it underestimates the  $^{40}\text{Ca}$  data by about 9%.

For  $^{12}\text{C}$  and  $^{16}\text{O}$  partial muon capture rates to particular bound levels have been also measured. We compare these data with our calculation in Table II. The calculated partial muon capture rates, as given in Table II, again reproduce the magnitude of these rates well, with the notable exception of the transition to the  $^{12}\text{B}$  ground state. It is well known that a proper description of this Gamow-Teller transition requires additional configuration mixing within the  $p$ -shell other than provided by the  $(1p-1h)$  RPA approach [14]. For the capture to the  $0^-$  and  $1^-$  states in  $^{16}\text{N}$  we performed the calculation not only by the continuum RPA, but also by the standard RPA which treats all states as bound; the two methods agree with each other quite well. For the  $2^-$  state we used only the latter method since the continuum RPA gives a much too narrow resonance in this case and the round-off errors are too severe.

Figure 1 shows the total  $^{12}\text{C}(\mu^-, \nu_\mu)^{12}\text{B}$  capture rate as a function of neutron energy  $E_N$  above the  $n + ^{11}\text{B}$  threshold in  $^{12}\text{B}$ . Most of this rate goes via  $1^-$  and  $2^-$  multipole excitations to the giant dipole and spin-dipole resonances. This is demonstrated in Fig. 1, which, as additional information, shows the partial contributions of these multipoles. Giant dipole and spin-dipole excitations also dominate the capture rates for the other two nuclei,  $^{16}\text{O}$  and  $^{40}\text{Ca}$ . For example, we find that the  $1^-$  and  $2^-$  multipoles together contribute about 75% [65%] to the total  $^{16}\text{O}(\mu^-, \nu_\mu)^{16}\text{N}$  [ $^{40}\text{Ca}(\mu^-, \nu_\mu)^{40}\text{K}$ ] rate. Excitation of the giant quadrupole resonance at about 20 MeV (see Fig. 1) contributes a few percent. For  $^{40}\text{Ca}$ , the  $0^-$  and  $3^-$  multipoles each contribute about 10% to the rate.

In accordance with our discussion above, we find an average excitation energy which in all cases corresponds to the regime of the giant dipole and spin-dipole resonances in these nuclei. If we consider the  $Q$ -values of the reactions, these average energies indicate that the average neutrino energy after the capture process is  $\langle E_\nu \rangle \simeq 80$  MeV, while the remaining 25 MeV of the muon mass are transferred, on average, to internal nuclear degrees of freedom.

In Fig. 2, we compare the excitation spectrum for the  $^{16}\text{O}(\mu^-, \nu_\mu)^{16}\text{N}$  reaction as calculated for the two residual interactions we used. Both spectra are very similar, but the Bonn potential predicts a slightly higher excitation rate to the giant dipole resonances, which accounts for the 10% difference in the total rates for the two interactions. Finally, in Fig. 3 we show the capture rate for  $^{40}\text{Ca}(\mu^-, \nu_\mu)^{40}\text{K}$  as a function of the excitation energy in the final nucleus  $^{40}\text{K}$ , i.e., for the whole range of the nuclear response.

All results presented so far have been obtained using the *free* nucleon form factors. To test the dependence of the calculated rates we repeated our muon capture calculations, however, using renormalized values for  $g_A$  and  $g_P$ . We present the results in Table III for three models of the in-medium renormalization. In model 1 we simply quench the axial vector coupling, and keep the Goldberger-Treiman relation intact:

$$\tilde{g}_p = \frac{2m_\mu M_p \tilde{g}_A}{m_\pi^2 - q^2}, \quad \tilde{g}_A = 1.0. \quad (3)$$

In models 2 and 3 we modify the relation between  $g_P$  and  $g_A$ , using the relation  $g_A = f_\pi g_{\pi NN}/M_p$  and two alternative prescriptions given in Ref. [6]. So in model 2

$$\tilde{g}_p = \frac{2m_\mu f_\pi \tilde{g}_{\pi NN}}{1.35(m_\pi^2 - q^2) - 0.35\vec{q}^2}, \quad \tilde{g}_{\pi NN}/g_{\pi NN} = 1.0/1.25, \quad \tilde{g}_A = 1.0, \quad (4)$$

and in model 3

$$\tilde{g}_p = \frac{0.6m_\mu f_\pi \tilde{g}_{\pi NN}}{m_\pi^2 - q^2 - 0.7\vec{q}^2}, \quad \tilde{g}_{\pi NN}/g_{\pi NN} = 1.0/1.25, \quad \tilde{g}_A = 1.0. \quad (5)$$

As expected from the axial vector dominance of the muon capture cross section, the rates in all three cases displayed in Table III are significantly smaller than the ones obtained for the free nucleon form factors. Depending on the adopted model for the renormalization, the rates are lowered by 20–30%, where the decrease is nearly the same for all three nuclei for a given model. This decrease clearly shows that the muon capture rate, although dominated by the axial vector current interaction, is also affected by the vector-axial vector interference, and by terms containing  $g_P$ . The induced pseudoscalar coupling decreases the capture rate, as one can see best in model 3 where  $g_P$  is strongly reduced. Comparing the three models

of renormalization we confirm the known weak sensitivity of the total capture rate to the variations in  $g_P$ . However, most importantly, the rates obtained with the quenched form factors are in disagreement with the data.

To test the sensitivity of our results to the adopted residual interaction we have performed calculations for all three nuclei, in which the overall strength of the Landau-Migdal force has been decreased or increased by 10%. In all of the calculations  $g_A$  was set to  $g_A = 1.25$ . Noting that the residual interaction is repulsive in the isovector channel and pushes the  $T = 1$  strength to higher excitation energies, a weakening of the force results in the  $T = 1$  states, which are the only states populated in muon capture on  $T = 0$  targets like  $^{12}\text{C}$ ,  $^{16}\text{O}$ , and  $^{40}\text{Ca}$ , residing at lower excitation energies. Consequently, the energy of the neutrinos  $E_\nu$ , which are released after the capture to these states, are slightly higher. As the muon capture rate is proportional to  $E_\nu^{2(1+\lambda)}$  ( $\lambda$  is the order of the spherical Bessel function of the corresponding operator) [1], it is increased when the residual interaction is weakened. The same sequence of arguments shows that the rate is lowered if the interaction is increased. These expectations are confirmed by our calculations. For example, the total muon capture rate on  $^{40}\text{Ca}$  is changed to  $22.77 \times 10^5 \text{ s}^{-1}$  ( $24.18 \times 10^5 \text{ s}^{-1}$ ) if the overall strength of the Landau-Migdal is increased (decreased) by 10%. When compared to our results, given in Table I, we conclude that a 10% variation in the interaction results in a change of the total muon capture rate of less than 3%. The same sensitivity is observed for the nuclei  $^{12}\text{C}$  and  $^{16}\text{O}$ , where the same variation in the interaction changes the rate by less than 3% and 2%, respectively. We conclude that the changes in the muon capture rates induced by the in-medium renormalization of the form factors  $g_A$  and  $g_P$  are noticeably larger than its sensitivity to reasonable variations of the residual interaction.

Before drawing conclusions from our calculations, it is perhaps worthwhile to briefly review other calculations of the muon capture rate for the nuclei we are considering. In the classical paper of Foldy and Walecka [15], the authors relate the dipole capture rate to the experimental photo-absorption cross section. In addition, they use symmetry arguments to relate the vector and axial vector nuclear matrix elements. In its slightly more modern

version [1], which uses the present free nucleon coupling constants, the calculation gives total capture rates quite close to ours in Table I for  $^{12}\text{C}$  and  $^{16}\text{O}$ , and perhaps 20% higher than our numbers (and the experiment) for  $^{40}\text{Ca}$ .

Another calculation worth mentioning is the treatment of  $^{16}\text{O}$  by Eramzhyan *et al.* [16]. This calculation employs a truncated shell model with ground state correlations included and standard free nucleon coupling constants. For the bound states in  $^{16}\text{N}$  the results are similar to ours in Table II, particularly to our entries for the Landau-Migdal force. For the transitions to unbound states (which the authors treat as shell model, i.e., bound anyway) they obtain a total capture rate of  $1.02 \times 10^5$  s, within 10% of our result. On the other hand, Ohtsuka's [17] calculated capture rates in  $^{12}\text{C}$  and  $^{16}\text{O}$  are larger than ours and the experiment by a substantial factor of 1.5 and 2.5, respectively. The author attributes this overestimate to the neglect of ground state correlations in the adopted nuclear model. In fact, the same calculation overestimates the photo-reaction cross section, which has nothing to do with weak interactions or axial vector current, by a similar factor.

All of these calculations are therefore basically compatible with our result, and suggest that the experimental rate is best reproduced with the free nucleon coupling constants. A similar conclusion follows from the comparison of the measured  $^{12}\text{C}(\nu_e, e^-)^{12}\text{B}^*$  cross sections for the  $\nu_e$  from stopped muon decay [18], with the results calculated within the same approach as employed here [19].

In contrast, the recent calculation in Ref. [20] is performed quite differently. It uses an approach based on the local density approximation to the infinite nuclear matter. In Ref. [20], the capture rate is reduced by a factor of about two by the strong nuclear renormalization. This renormalization seems to include both the effects of residual interaction, which reduce the rate as we argued above, and the effect of in-medium renormalization. It is difficult to separate the two, and therefore difficult to compare our results with those of Ref. [20].

Our calculations show that the continuum RPA method with a standard, unadjusted residual interaction describes the muon capture rates in the  $T = 0$  nuclei quite well, pro-

vided that free nucleon form factors are used. In particular, quenching of the axial current coupling constant suggested in the analysis of the Gamow-Teller strength would result in a noticeable disagreement with the data. We checked that this conclusion is not sensitive to reasonable variation in the residual force. We stress that the muon capture is dominated by the transitions to the negative parity dipole and spin-dipole collective states. Our conclusion is therefore only relevant for such states.

#### **ACKNOWLEDGMENTS**

We would like to thank Professor Magda Ericson for discussions, in particular about the role of the pseudoscalar coupling. This work was supported in part by the National Science Foundation, Grant No. PHY91-15574, and by the U.S. Department of Energy, Contract #DE-F603-88ER-40397.

## REFERENCES

- [1] J. D. Walecka in *Muon Physics II*, edited by V.W. Hughes and C. S. Wu (Academic Press, NY, 1975) p. 113.
- [2] N. C. Mukhopadhyay, Phys. Rep. **30C**, 1 (1977).
- [3] B. H. Wildenthal, Progr. Part. Nucl. Phys. **11**, 5 (1984).
- [4] C. D. Goodman and S. B. Bloom, in *Spin Excitations in Nuclei*, edited by F. Petrovich *et al.* (Plenum, New York, 1983) p. 143; G. F. Bertsch and H. Esbensen, Rep. Prog. Phys. **50**, 607 (1987); O. Häusser *et al.*, Phys. Rev. C **43**, 230 (1991).
- [5] M. L. Goldberger and S. B. Treiman, Phys. Rev. **111**, 354 (1958).
- [6] J. Delorme and M. Ericson, to be published.
- [7] M. Buballa, S. Drozdz, S. Krewald, and J. Speth, Ann. Phys. **208**, 346 (1991); E. Kolbe, K. Langanke, S. Krewald, and F. K. Thielemann, Nucl. Phys. **A540**, 599 (1992).
- [8] K. Nakayama, S. Drozdz, S. Krewald, and J. Speth, Nucl. Phys. **A470**, 573 (1987).
- [9] R. Machleidt, K. Holinde, and Ch. Elster, Phys. Rep. **149**, 1 (1987).
- [10] G. Co and S. Krewald, Nucl. Phys. **A433**, 392 (1985).
- [11] M. Buballa *et al.*, Nucl. Phys. **A517**, 61 (1990).
- [12] S. Krewald, K. Nakayama, and J. Speth, Phys. Rep. **161**, 103 (1988).
- [13] E. J. Beise and R. D. McKeown, Comments Nucl. Part. Phys. **20**, 105 (1991).
- [14] W. T. Chou, E. K. Warburton, and B. A. Brown, Phys. Rev. C **47**, 163 (1993).
- [15] L. L. Foldy and J. D. Walecka, Il Nuovo Cimento **34**, 1026 (1964).
- [16] R. A. Eramzhyan, M. Gmitro, R. A. Sakaev, and L. A. Tosunjan, Nucl. Phys. **A290**, 294 (1977).

- [17] N. Ohtsuka, Nucl. Phys. **A370**, 431 (1981).
- [18] J. Kleinfellner *et al.*, KARMEN collaboration, in Proceedings of the XIII International Conference on Particles and Nuclei, Perugia, Italy, 1993, edited by A. Pascolini.
- [19] E. Kolbe, K. Langanke, and S. Krewald, Phys. Rev. C **49**, 1122 (1994).
- [20] H. C. Chiang, E. Oset, and P. Fernandez de Cordoba, Nucl. Phys. **A510**, 591 (1990).
- [21] T. Suzuki, D. F. Measday, and J. P. Roalsvig, Phys. Rev. C **35**, 2212 (1987).
- [22] Y. G. Budgashov *et al.*, JETP **31**, 651 (1970).
- [23] M. Giffon *et al.*, Phys. Rev. C **24**, 241 (1981).
- [24] G. H. Miller, M. Eckhause, F. R. Kane, P. Martin, and R. E. Welsh, Phys. Lett. **41B**, 50 (1972).
- [25] L. Ph. Roesch *et al.*, Phys. Lett. **107B**, 31 (1981).
- [26] R. C. Cohen, S. Devons, and A. D. Canaris, Nucl. Phys. **57**, 255 (1964).
- [27] A. Astbury *et al.*, Nuovo Cimento **33**, 1020 (1964).
- [28] J. P. Deutsch *et al.*, Phys. Lett. **29B**, 66 (1969).
- [29] F. R. Kane *et al.*, Phys. Lett. **45B**, 292 (1973).

## FIGURES

FIG. 1. Muon capture in  $^{12}\text{C}$  as a function of the neutron energy  $E(n)$ . Full line is the total rate, dashed line is for the  $1^-$  multipole, short dashed line is for the  $2^-$  multipole, and the dotted line is for the  $2^+$  multipole. The calculation is for the Landau-Migdal interaction.

FIG. 2. Muon capture in  $^{16}\text{O}$ . Full line is the capture rate for the Bonn potential and the dashed line is for the Landau-Migdal force.

FIG. 3. Muon capture rate in  $^{40}\text{Ca}$  as a function of the excitation energy in the final nucleus  $^{40}\text{K}$ . The calculation is for the Landau-Migdal force.

## TABLES

TABLE I. Comparison of calculated total muon capture rates with experimental data [21]. For  $^{12}\text{C}$  and  $^{16}\text{O}$  the capture rates to particle-bound states have been subtracted. The rates are given in  $10^5 \text{ s}^{-1}$ .

Target nucleus	Experiment	Bonn potential	Landau-Migdal potential
$^{12}\text{C}$	$0.320 \pm 0.01$	0.342	0.334
$^{16}\text{O}$	$0.924 \pm 0.01$	0.969	0.919
$^{40}\text{Ca}$	$25.57 \pm 0.14$	26.2	23.4

TABLE II. Partial muon capture rates for the bound states in  $^{12}\text{C}(\mu^-, \nu_\mu)^{12}\text{B}^*$  (upper part) and  $^{16}\text{O}(\mu^-, \nu_\mu)^{16}\text{N}^*$  (lower part) in units of  $s^{-1}$ , calculated for the Landau-Migdal force (LM) and the Bonn potential (BP). In each part the theoretical results are shown in the top two lines, followed by the measured data. Note, that the values marked with  $\#$  were assumed to be 0, as the  $0^+ \rightarrow 2^+$  transition is second-forbidden.

Source	$\omega(1^+)$	$\omega(1^-)$	$\omega(2^-)$	$\omega(2^+)$
(LM)	25400	220	40	$\leq 1$
(BP)	22780	745	25	$\leq 1$
Ref. [22]	$6290 \pm 300$	$720 \pm 175$	$10 \pm 230$	$0^\#$
Ref. [23]		$1080 \pm 125$	$60 \pm 200$	$0^\#$
Ref. [24]	$6000 \pm 400$	$890 \pm 100$	$170 \pm 240$	$0^\#$
Ref. [24]	$5700 \pm 800$	$700 \pm 400$	$400 \pm 600$	$200 \pm 400$
Ref. [25]	$6280 \pm 290$	$380 \pm 100$	$120 \pm 80$	$270 \pm 100$

Source	$\omega(0^-)$	$\omega(1^-)$	$\omega(2^-)$
(LM)	1.45	1.75	8.10
(BP)	1.85	3.10	8.65
Ref. [26]	$1.1 \pm 0.2$	$1.9 \pm 0.1$	$6.3 \pm 0.7$
Ref. [27]	$1.6 \pm 0.2$	$1.4 \pm 0.2$	
Ref. [28]	$0.85 \pm 0.06$	$1.85 \pm 0.17$	
Ref. [29]	$1.56 \pm 0.17$	$1.31 \pm 0.1$	$8.2 \pm 1.2$

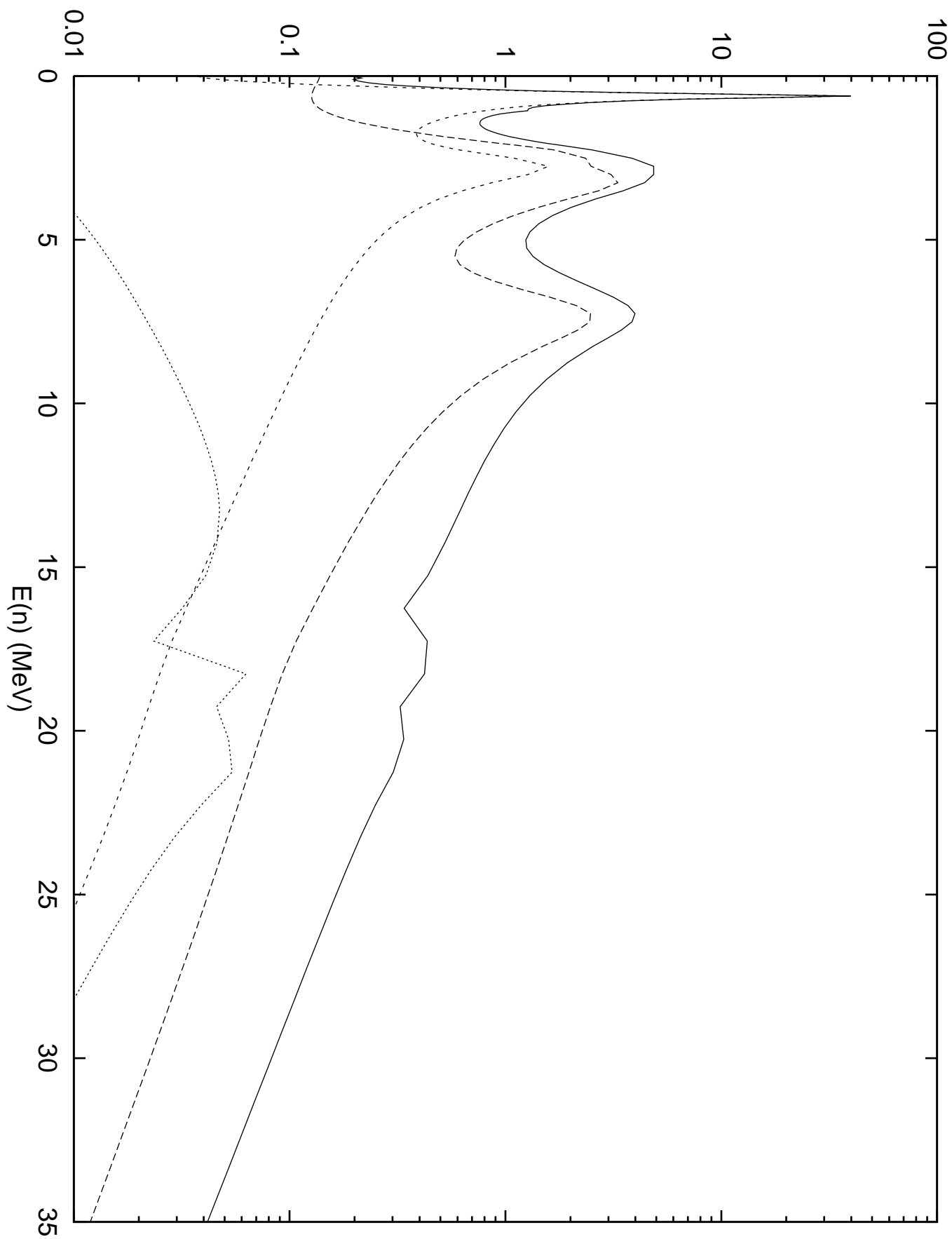
TABLE III. Same as Table I, but calculated for the three renormalization models of  $g_A$  and  $g_P$ , defined in Eqs. (3-5). The calculations have been performed for the Landau-Migdal force. The rates are given in  $10^5$  s $^{-1}$ .

Target nucleus	Experiment	Model 1	Model 2	Model 3
$^{12}\text{C}$	$0.320 \pm 0.01$	0.245	0.252	0.267
$^{16}\text{O}$	$0.924 \pm 0.01$	0.682	0.698	0.736
$^{40}\text{Ca}$	$25.57 \pm 0.14$	17.3	17.8	18.8

This figure "fig1-1.png" is available in "png" format from:

<http://arxiv.org/ps/nucl-th/9405030v1>

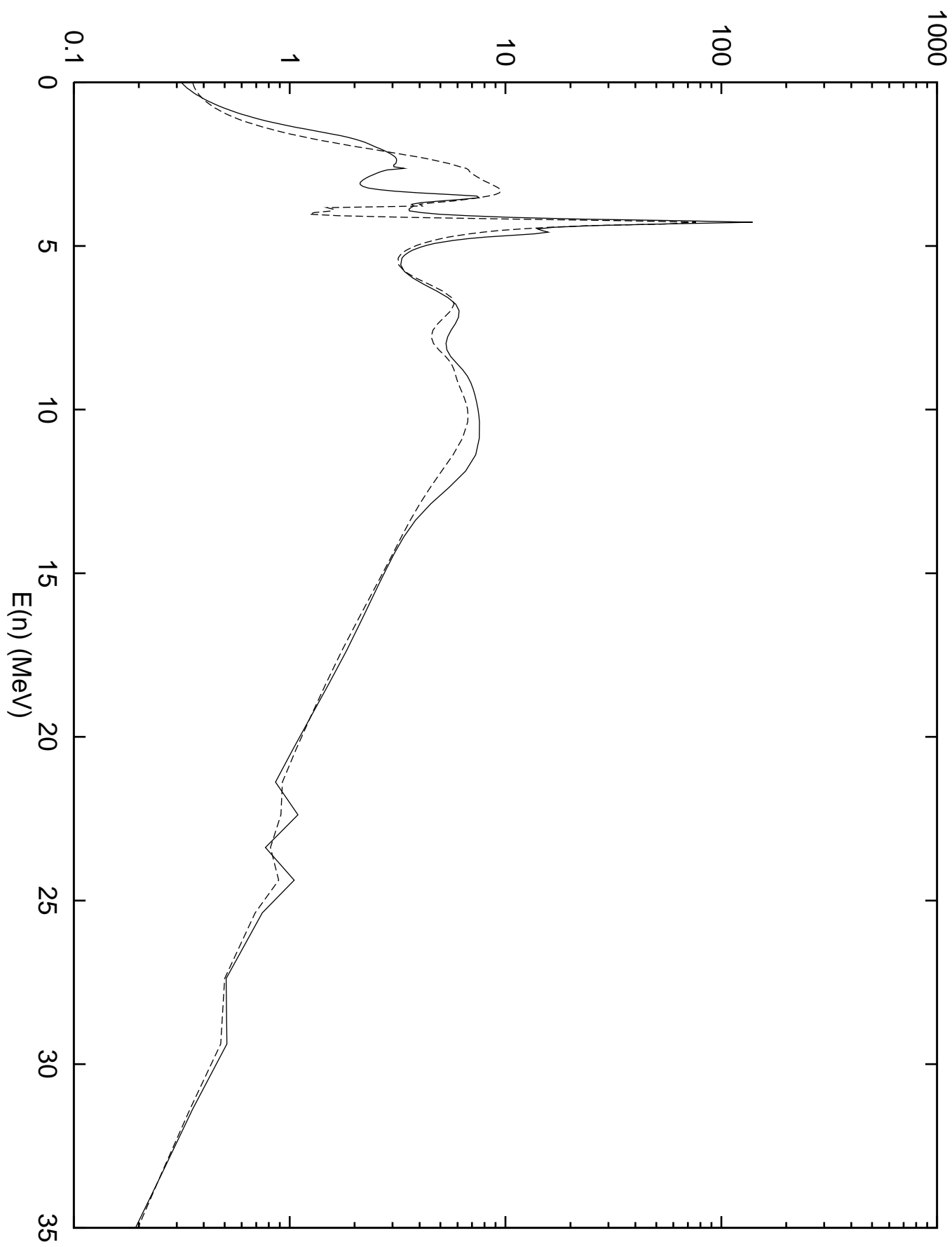
differential capture rate in  $1000/(s \text{ MeV})$



This figure "fig1-2.png" is available in "png" format from:

<http://arxiv.org/ps/nucl-th/9405030v1>

differential capture rate in  $1000/(s \text{ MeV})$



This figure "fig1-3.png" is available in "png" format from:

<http://arxiv.org/ps/nucl-th/9405030v1>

